

Trenched epitaxial lateral overgrowth of fast coalesced a-plane GaN with low dislocation density

Te-Chung Wang, Tien-Chang Lu, Tsung-Shine Ko, Hao-Chung Kuo, Min Yu, Sing-Chung Wang, Chang-Cheng Chuo, Zheng-Hong Lee, and Hou-Guang Chen

Citation: *Applied Physics Letters* **89**, 251109 (2006); doi: 10.1063/1.2405880

View online: <http://dx.doi.org/10.1063/1.2405880>

View Table of Contents: <http://scitation.aip.org/content/aip/journal/apl/89/25?ver=pdfcov>

Published by the AIP Publishing

Articles you may be interested in

[Nanorod epitaxial lateral overgrowth of a-plane GaN with low dislocation density](#)

Appl. Phys. Lett. **94**, 251912 (2009); 10.1063/1.3158954

[Epitaxial lateral overgrowth of a-plane GaN by metalorganic chemical vapor deposition](#)

J. Appl. Phys. **102**, 053506 (2007); 10.1063/1.2773692

[Defect reduction in \(112̄0\) a-plane GaN by two-stage epitaxial lateral overgrowth](#)

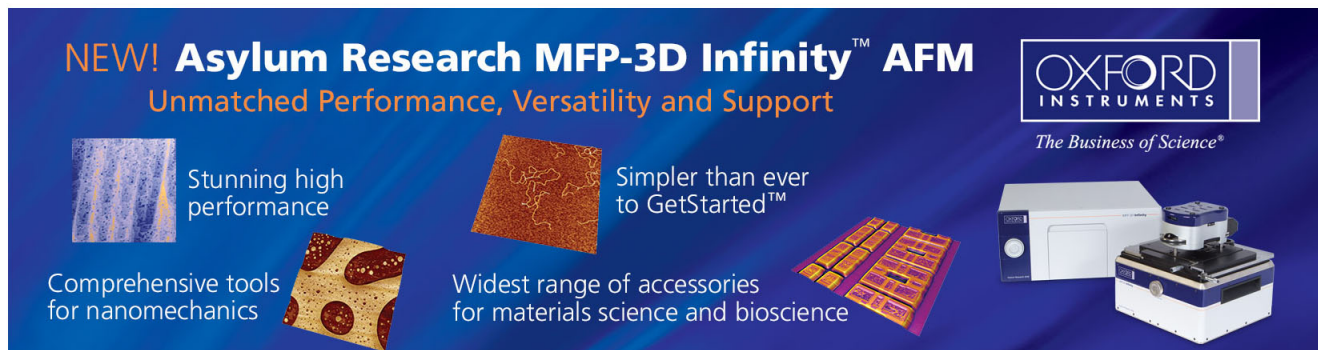
Appl. Phys. Lett. **89**, 262105 (2006); 10.1063/1.2423328

[Defect reduction in nonpolar a-plane GaN films using in situ SiNx nanomask](#)

Appl. Phys. Lett. **89**, 041903 (2006); 10.1063/1.2234841

[Correlation of strain, wing tilt, dislocation density, and photoluminescence in epitaxial lateral overgrown GaN on SiC substrates](#)

J. Appl. Phys. **96**, 3666 (2004); 10.1063/1.1784617

The advertisement features a dark blue background with white and orange text. At the top left, it reads 'NEW! Asylum Research MFP-3D Infinity™ AFM' in large white letters, followed by 'Unmatched Performance, Versatility and Support' in orange. On the right, the Oxford Instruments logo is shown with the tagline 'The Business of Science®'. Below the text are four images: a blue textured surface, a brown textured surface, a yellow and red patterned surface, and a photograph of the MFP-3D Infinity AFM instrument. Text descriptions are placed around these images: 'Stunning high performance' next to the blue surface, 'Simpler than ever to GetStarted™' next to the brown surface, 'Comprehensive tools for nanomechanics' next to the patterned surface, and 'Widest range of accessories for materials science and bioscience' next to the instrument photo.

Trenched epitaxial lateral overgrowth of fast coalesced *a*-plane GaN with low dislocation density

Te-Chung Wang, Tien-Chang Lu,^{a),b)} Tsung-Shine Ko, Hao-Chung Kuo,^{a),c)}
Min Yu, and Sing-Chung Wang

Department of Photonics and Institute of Electro-Optical Engineering, National Chiao Tung University,
Hsinchu, Taiwan 300, ROC

Chang-Cheng Chuo and Zheng-Hong Lee

Electronics and Optoelectronics Research Laboratories, Industrial Technology Research Institute, Dashi
Township, Kaohsiung County 840, Taiwan, ROC

Hou-Guang Chen

Department of Materials Science and Engineering, I-Shou University, Hsinchu, Taiwan 310, ROC

(Received 29 August 2006; accepted 9 November 2006; published online 19 December 2006)

The crystal quality of *a*-plane GaN films was improved by using epitaxial lateral overgrowth on trenched *a*-plane GaN buffer layers. Not only the threading dislocation density but also the difference of anisotropic in-plane strain between orthogonal crystal axes can be mitigated by using trenched epitaxial lateral overgrowth (TELOG). The low threading dislocation density investigated by the cross-sectional transmission electron microscopy was estimated to be $3 \times 10^7 \text{ cm}^{-2}$ on the N-face GaN wing. On the other hand, the Ga-face GaN wing with a faster lateral overgrowth rate could be influenced by the thin GaN layer grown on the bottom of the trenches, resulting in higher dislocation density generated. As a result, the authors concluded that a narrower striped GaN seeds and deeper striped trenches etched into the surface of sapphire could derive a better quality *a*-plane GaN film. Finally, they demonstrated the fast coalescence process of TELOG GaN films below $10 \mu\text{m}$ thick. © 2006 American Institute of Physics. [DOI: 10.1063/1.2405880]

The radiative quantum efficiency of nitride light emitters grown along $[0001]$ *c* direction is low due to the presence of built-in electric fields, by the spontaneous and piezoelectric polarizations separating the electron and hole spatial distributions to incline the band structure and reduce oscillator strength in the quantum wells.¹ Since the performances of III-nitride devices are limited by the polarization-related internal electric fields, nonpolar GaN is currently the subject of intense research due to the potential to improve the internal quantum efficiency of GaN optoelectronic devices. To eliminate such polarization effects, growth along nonpolar orientations has been, respectively, explored for $[11\bar{2}0]$ *a*-plane GaN on $[10\bar{1}2]$ *r*-plane sapphire² and *a*-plane SiC,³ and $[10\bar{1}0]$ *m*-plane GaN on $[100]$ LiAlO₂ substrates.^{4,5} However, nonpolar *a*-plane GaN based material grown on *r*-plane sapphire substrates always accompanies with a wavy, stripe-like growth feature and possess a large density of threading dislocations and stacking faults. In addition, the lattice mismatch between *a*-plane GaN and *r*-plane sapphire results in serious anisotropic in-plane strain difference between orthogonal crystal axes.⁶ Recently, successful epitaxial lateral overgrowth (ELOG) of *a*-plane GaN on *r*-plane sapphire has been reported,⁷ which significantly improves the material quality by reducing the density of threading dislocations and alleviates the strain-related surface roughening and faceting.⁷ Despite the ELOG assisted morphology and quality improvements in *a*-plane GaN over *r*-plane sapphire, the coalescence thickness, usually more than $20 \mu\text{m}$, is quiet thick and difficult to control the uniformity. In this letter, we improve

$[11\bar{2}0]$ *a*-plane GaN quality by using epitaxial lateral overgrowth on trenched *a*-plane GaN buffer layers. The trenched epitaxial lateral overgrowth (TELOG) allowed us to obtain *a*-plane GaN with low dislocation density, simple fabrication process, lower cost, and thinner coalescence thickness in comparisons to the previous reports.

Figure 1 shows the flow chart to grow the TELOG *a*-GaN. First, the *a*-plane GaN templates with $1.5 \mu\text{m}$ thickness were grown by low pressure metal-organic chemical vapor deposition (MOCVD) on *r*-plane Al₂O₃ sapphire substrates using conventional two-step growth technique. Then, a $2 \mu\text{m}$ seed/ $18 \mu\text{m}$ trench TELOG stripe pattern was applied parallel to the $[1\bar{1}00]$ direction to realize vertical *c*-plane sidewalls followed by etching of SiO₂ using inductively coupled plasma etching through the windows to the GaN epitaxial film. GaN stripes were etched through the mask openings, down to the *r*-plane sapphire substrate by

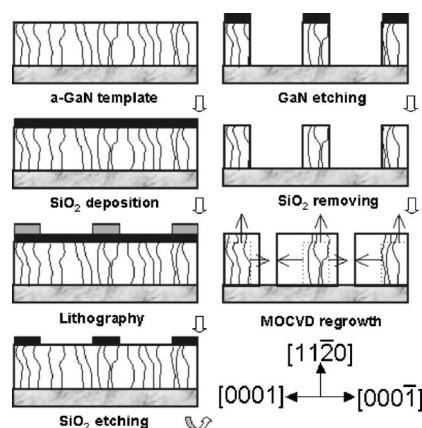


FIG. 1. Flow chart of *a*-plane GaN TELOG process.

^{a)} Author to whom correspondence should be addressed.

^{b)} Electronic mail: timclu@faculty.nctu.edu.tw

^{c)} Electronic mail: hckuo@faculty.nctu.edu.tw

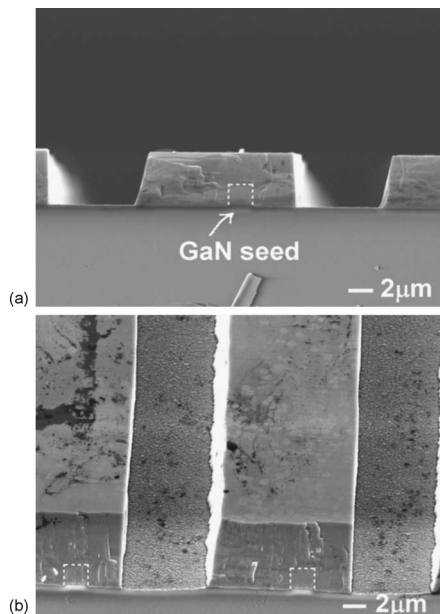


FIG. 2. Cross-sectional SEM of the uncoalesced TELOG *a*-plane GaN film with 2 μm seed/18 μm trench pattern.

reactive ion etching. To simplify the growth process, the SiO_2 mask was removed by hydrofluoric acid followed by depositing *a*-plane GaN TELOG film using a single-step growth process. In this study, the growth temperature, pressure, and V/III ratio were 1190 $^\circ\text{C}$, 100–150 mbars, and 700–800, respectively. The grown samples were investigated by scanning electron microscopy (SEM), high-resolution x-ray diffraction, and transmission electron microscopy (TEM). We also used a scanning optical microscopy to scan a $25 \times 25 \mu\text{m}^2$ microphotoluminescence ($\mu\text{-PL}$) mappings with spatial and spectral resolutions of 1 μm and 1 nm, respectively, pumped by a He–Cd laser operating on 325 nm with 25 mW.

To observe the growth mechanism, we stopped the process before the coalescence of the GaN films. The SEM images of cross-sectional and birds-view TELOG GaN by MOCVD were shown in Fig. 2(a). The growth rate of the Ga-face wing was twice faster than the N-face wing. However, the ratio of growth rate in Ga-face wing to N-face wing was not as high as an order of magnitude reported by Imer *et al.*⁸ A thin GaN layer about 0.2 μm grown on the bottom of the trenches, as shown in Fig. 2(b), could be the reason to hinder the lateral growth rate in the Ga-face wing and hence affect the epitaxial quality.

High-resolution x-ray rocking curves along $[0001]$ *c* and $[1\bar{1}00]$ *m* directions were shown in Fig. 3. The full width at half maximum (FWHM) of x-ray rocking curves for an as-grown *a*-GaN 1.5 μm bulk layer in $[1\bar{1}00]$ direction is almost twice as large as that in $[0001]$ direction. It shows that the strains between the orthogonal crystal axes, *c*-axis and *m*-axis, are quite different and enhance the formation of line defects. Moreover, the surface geometry could show a wavy, stripelike growth feature if the nucleation layer was not optimized or the epitaxial film was thick.² However, after lateral overgrowth, the stresses of TELOG layer were released in both *c* axis and *m* axis and thus the crystal quality was enhanced especially in the $[1\bar{1}00]$ direction. As shown in Fig. 3, the FWHM of x-ray rocking curves for a TELOG layer was reduced from 1811 to 352 arc sec. Since the strip of the

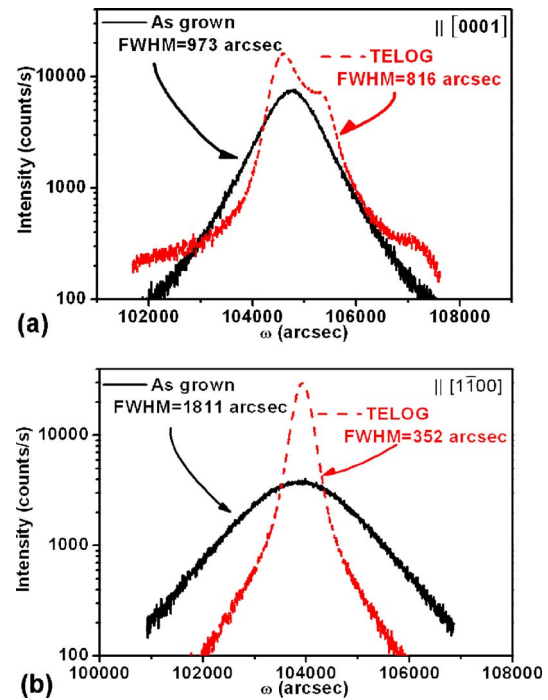


FIG. 3. (Color online) X-ray rocking curves of as-grown and TELOG *a*-plane GaN films (a) along $[0001]$ direction (b) along $[1\bar{1}00]$ direction.

TELOG layer did not coalesce, we observed obvious wing tilt phenomenon along $[0001]$ direction leading to the broadening effect of the x-ray rocking curve. Unlike the symmetric wing tilt in *c*-plane ELOG GaN,^{9,10} the wing tilt in *a*-plane TELOG GaN is asymmetric shown in the x-ray rocking curve, resulting from the different lateral growth rates of the window GaN in the $[0001]$ and the $[000\bar{1}]$ directions.^{7,11} Although the FWHM of x-ray rocking curves for a TELOG layer was only reduced from 973 to 816 arc sec, the crystal quality would be better as the TELOG film fully coalesced to lessen wing tilt phenomenon.

Figure 4(a) shows a $\mu\text{-PL}$ mapping of *a*-plane TELOG stripes. As shown in Fig. 4(a), five different regions can be distinguished in the TELOG sample and were labeled with numbers 1–5. Comparing the $\mu\text{-PL}$ mapping with the SEM image, region 5 showing the lowest $\mu\text{-PL}$ intensity area can be identified as the uncoalesced trenched region since *a*-GaN grown on *r* sapphire without a nucleation layer showed a textured surface with worst crystal quality. On the other hand, region 1 showing the strongest $\mu\text{-PL}$ intensity area can be identified as the N-face GaN wing. Region 2 is the stripped *a*-GaN seed. Regions 3 and 4 belong to the Ga-face GaN wing. Interestingly, region 3 standing at the initial region of the Ga-face GaN wing shows a higher PL intensity than that in region 4.

The distributions and types of dislocations were investigated by cross-sectional TEM shown in Figs. 4(b) and 4(c). According to the $g=(0002)$ and $g=(11\bar{2}0)$ two beam bright field images, most of the threading dislocations are obvious in both of the $g=(11\bar{2}0)$ and (0002) two beam conditions, indicating that these dislocations are mixed *a+c* type dislocations. The distribution of dislocations in Figs. 4(b) and 4(c) can also be labeled with numbers 1–5 fully corresponding to the $\mu\text{-PL}$ mapping results. The threading dislocation densities (TDDs) of stripped GaN seed in region 2 was more than $1 \times 10^{10} \text{ cm}^{-2}$. TDD of Ga-face GaN wing in region 4 was

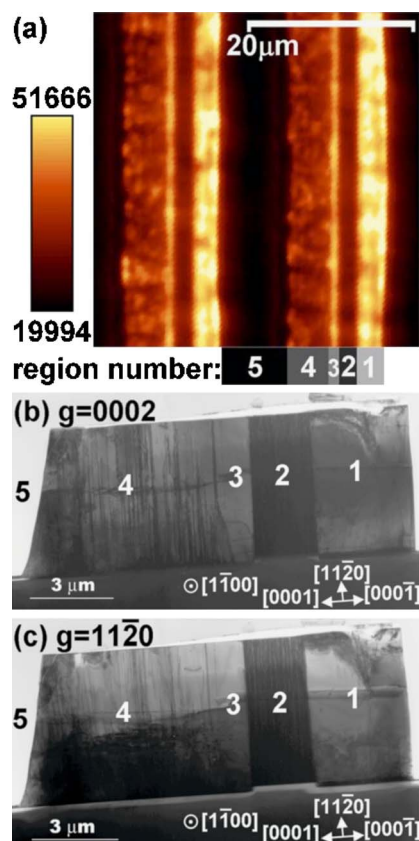


FIG. 4. (Color online) (a) Top view μ -PL image of TELOG *a*-plane GaN film. [(b) and (c)] Cross-sectional TEM $g=(0002)$ and $g=(11\bar{2}0)$ two beam bright field images.

about $9 \times 10^9 \text{ cm}^{-2}$ and TDD of N-face GaN wing in region 1 was about $3 \times 10^7 \text{ cm}^{-2}$, three orders of magnitude lower than planar films. The lower dislocation density in region 3 in comparison to region 4 was in accordance with a higher PL intensity. Because the lateral growth mode could be affected when the laterally grown layers encounters the underlying GaN layers, we suggest that the crystal quality of Ga-face GaN with a higher growth rate could be easily affected by the thin *a*-GaN layer grown on the bottom of the uncoalesced windows. Due to the relatively low growth rate of the thin *a*-GaN layer on the bottom of the trench, the crystal quality of the Ga-face GaN wing at the beginning of the lateral growth was good while the thin *a*-GaN layer was not formed, resulting in a low dislocation and high PL intensity area of region 3. According to the results of SEM image, the rough GaN layer grown on the window of TELOG without smooth nucleation layer is difficult to grow more than $0.2 \mu\text{m}$. As a result, to obtain a better crystal quality *a*-plane TELOG GaN for the most of the area, the trench depth shall be down to at least $0.2 \mu\text{m}$ deeper than the sapphire surface to prevent the coalescing between the TELOG layer and thin GaN layer.

We then continue to perform the TELOG process with a $2 \mu\text{m}$ seed / $18 \mu\text{m}$ trench stripe pattern to obtain a fully coalesced *a*-plane GaN film, as shown in the SEM image of Fig. 5. The coalescence process can fully be completed for the thickness around $10 \mu\text{m}$, it is a useful technique to overcome the thickness problem that the previous ELOG always needs more than $30 \mu\text{m}$ to fully coalesce.⁸ The FWHM of x-ray curves can be reduced to 385 arc sec in $[0001]$ and

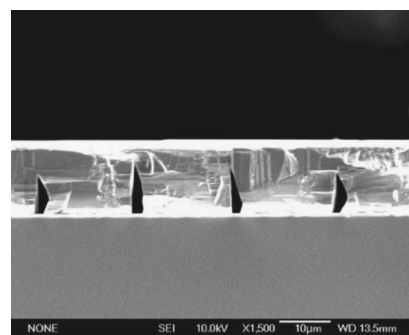


FIG. 5. Cross-sectional SEM of fully coalesced TELOG *a*-plane GaN film with $2 \mu\text{m}$ seed/ $18 \mu\text{m}$ trench pattern.

260 arc sec in $[1\bar{1}00]$ directions without wing tilt phenomenon demonstrating not only a high crystal quality but also an isotropic characteristic of *a*-plane TELOG GaN films.

In conclusion, we have grown high quality and fully coalesced *a*-plane GaN films at the thickness of $10 \mu\text{m}$ by using TELOG with a $2 \mu\text{m}$ seed/ $18 \mu\text{m}$ trench stripe pattern. The FWHMs of x-ray rocking curves along $[0001]$ *c* and $[1\bar{1}00]$ *m* directions were reduced from 973 to 385 arc sec and from 1811 to 260 arc sec, respectively, demonstrating the improvement of the crystal quality and the mitigation of the anisotropic in-plane strains between different crystal axes by TELOG. According to the results of μ -PL mapping and TEM, the TDD can be reduced largely from 1×10^{10} to $3 \times 10^7 \text{ cm}^{-2}$ for the N-face GaN wing. The Ga-face GaN could be much easily influenced by the thin GaN layer grown on the bottom of trench, indicating that a narrower stripped GaN seeds and deeper trench etched into the surface of sapphire can derive a better quality *a*-plane TELOG GaN film for the most of the area.

The authors would like to specially acknowledge the financial support by the Ministry of Economic Affairs, Taiwan, Republic of China, the MOE ATU program, and the National Science Council of Republic of China (ROC) in Taiwan under Contract Nos. NSC 94-2120-M-009-007 and NSC 94-2215-E-009-082.

¹P. Waltereit, O. Brandt, A. Trampert, H. T. Grahn, J. Menniger, M. Ramsteiner, M. Reiche, and K. H. Ploog, *Nature (London)* **406**, 865 (2000).

²M. D. Craven, S. H. Lim, F. Wu, J. S. Speck, and S. P. DenBaars, *Appl. Phys. Lett.* **81**, 469 (2002).

³M. D. Craven, A. Chakraborty, B. Imer, F. Wu, S. Keller, U. K. Mishra, J. S. Speck, and S. P. DenBaars, *Phys. Status Solidi C* **1**, 4 (2003).

⁴E. S. Hellman, Z. Liliental-Weber, and D. N. E. Buchanan, *MRS Internet J. Nitride Semicond. Res.* **2**, 30 (1997).

⁵P. Waltereit, O. Brandt, M. Ramsteiner, A. Trampert, H. T. Grahn, J. Menniger, M. Reiche, R. Uecker, P. Reiche, and K. H. Ploog, *Phys. Status Solidi A* **180**, 133 (2000).

⁶H. Wang, C. Chen, Z. Gong, J. Zhang, M. Gaevski, M. Su, J. Yang, and M. A. Khan, *Appl. Phys. Lett.* **84**, 499 (2004).

⁷M. D. Craven, S. H. Lim, F. Wu, J. S. Speck, and S. P. DenBaars, *Appl. Phys. Lett.* **81**, 1201 (2002).

⁸B. M. Imer, F. Wu, S. P. DenBaars, and J. S. Speck, *Appl. Phys. Lett.* **88**, 061908 (2006).

⁹P. Fini, H. Marchand, J. P. Ibbetson, S. P. DenBaars, U. K. Mishra, and J. S. Speck, *J. Cryst. Growth* **209**, 581 (2000).

¹⁰W. M. Chen, P. J. McNally, K. Jacobs, T. Tuomi, A. N. Danilewsky, Z. R. Zytkeiwicz, D. Lowney, J. Kanatharana, L. Knuutila, and J. Riikonen, *J. Cryst. Growth* **243**, 94 (2002).

¹¹C. Chen, J. Yang, H. Wang, J. Zhang, V. Adivarahan, M. Gaevski, E. Kuokstis, Z. Gong, M. Su, and M. Asif Khan, *Jpn. J. Appl. Phys., Part 2* **42**, L640 (2003).